Performance and Lyapunov Stability of a Nonlinear Path-Following Guidance Method

Hrishav Das
Reva Dhillon
Agni Ravi Deepa

7th November 2024

AS5570 Course Project Presentation (Group 1)

Contents

Problem Statement

The objective of the project is to discuss a nonlinear guidance method to accomplish trajectory following for unmanned air vehicles (UAVs).

The guidance method under consideration uses an imaginary point moving along the desired flight path as a pseudotarget to generate the lateral acceleration commands for controlling UAVs.

Performance and stability are demonstrated for this nonlinear path-following guidance method.

Motivation

Precise and accurate path following by UAVs is of prime importance, particularly in the following applications:

- Mapping
- Search and Rescue
- Patrol
- Surveillance

A factor of key importance in any guidance algorithm designed for the purpose of path following is the reaction of the UAV to wind disturbances. Each of the applications above requires that the UAV adapt to the wind.

Advantages

The nonlinear guidance law has a number of advantages over the other approaches for following curved paths. In particular, the law:

- Naturally follows any circular path of radius greater than a specific limit imposed by the dynamics of the vehicle.
- Has an element of anticipation of the desired flight path, enabling tight tracking of curved flight trajectories.
- Incorporates instantaneous vehicle speed, adding an adaptive feature with respect to changes in vehicle ground speed caused by external disturbances, such as wind. This makes its stability independent of vehicle velocity.
- Is asymptotically stable, for all velocities, in the entire state space of useful initial conditions, and in the presence of saturation limits on lateral acceleration.
- Is very simple and straightforward to apply in actual flight applications.

The Guidance Law

- A reference point on the desired path is designated, and a lateral acceleration command is generated according to the direction of the reference point relative to vehicle velocity.
- This reference point is at a fixed distance ($L1$) forward of the vehicle.
- The commanded acceleration is such that the vehicle follows an appropriate circle, passing through the vehicle's position and the reference point.

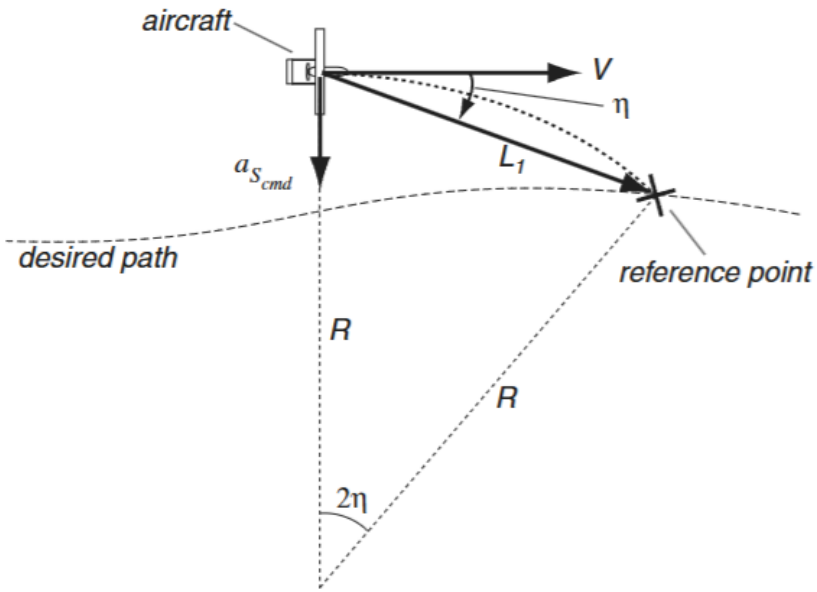

The Guidance Law

$$\boxed{a_{s_{cmd}} = 2\frac{V^2}{L_1}\sin\eta} \tag{1}$$

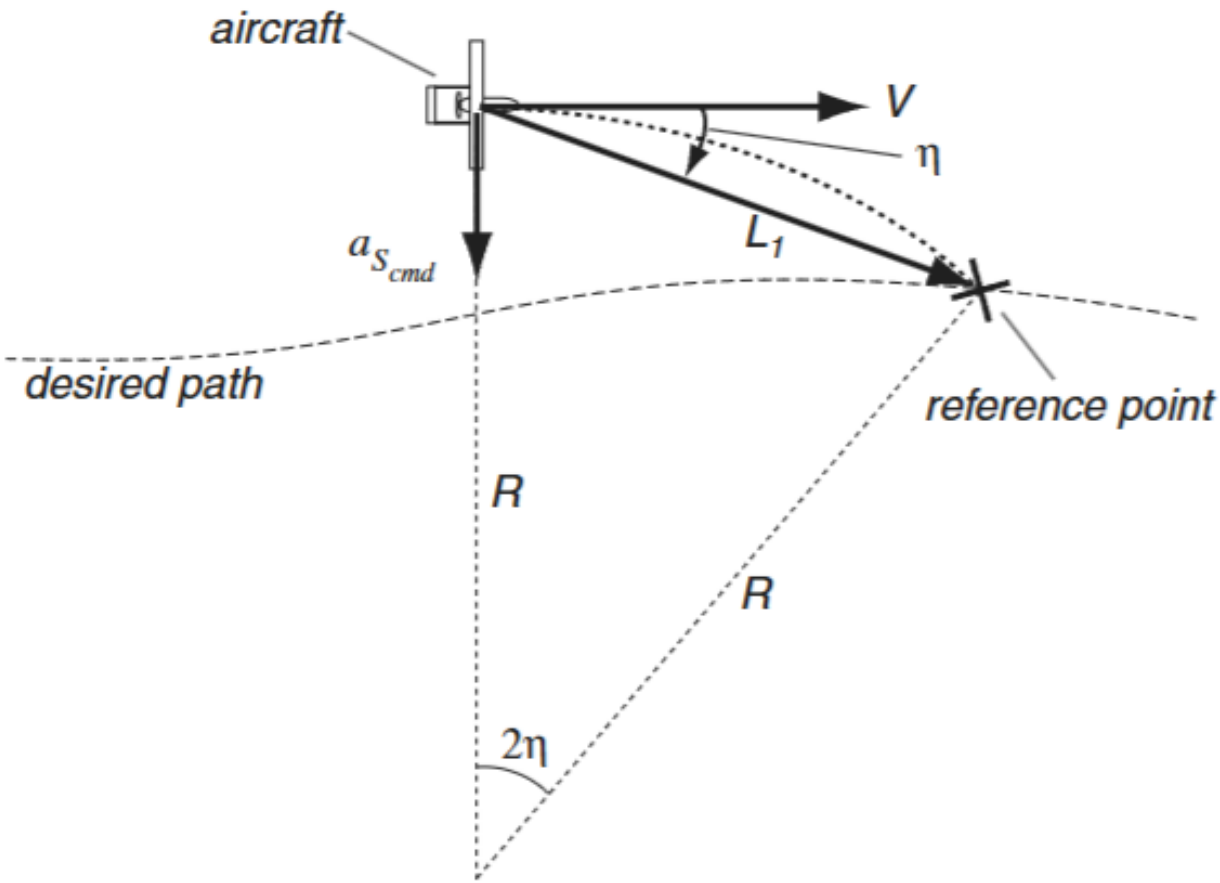

The Guidance Law

- The commanded lateral acceleration is the centripetal acceleration required by the vehicle to follow the above-mentioned instantaneous circle segment.
- The guidance method will tend to align the vehicle velocity direction with the direction of the L_1 line segment.
- If the vehicle is far away from the desired path, then the guidance method tends to rotate the velocity direction to approach the desired path at a large angle. On the other hand, if the vehicle is close to the desired path, then the guidance law rotates the velocity direction to approach the desired path at a small angle.

Relation to PN

- The lateral acceleration command in Eq (1) is similar to that encountered in PN (RTPN) with a navigation constant of $N = 2$, under the assumption that the reference point is stationary.

$$a_{\perp \mathrm{LOS}} = a_s \cos\eta = 2\frac{V^2}{L_1}\sin\eta\cos\eta = \boxed{2(\underbrace{V\cos\eta}_{V_c})\underbrace{\left(\frac{V}{L_1}\sin\eta\right)}_{-\dot{\theta}}}$$

- However, the reference point is actually moving along the reference trajectory, and with the L1 constant, the closing speed between the reference point and the vehicle is always zero.

Linear Analysis

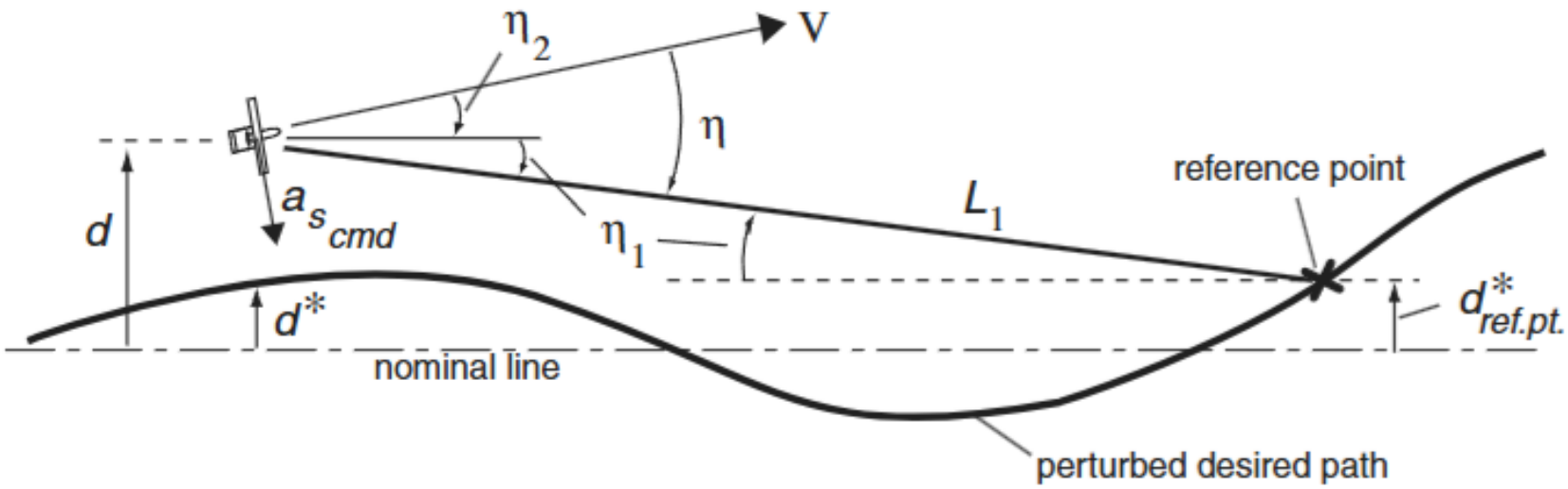

- $\sin\eta \approx \eta_1 + \eta_2$
- $\eta_1 \approx \frac{d - d_{ref}}{L_1}$
- $\eta_2 \approx \frac{\dot{d}}{V}$
- $a_{s_{cmd}} \approx -\ddot{d}$

Linear Analysis

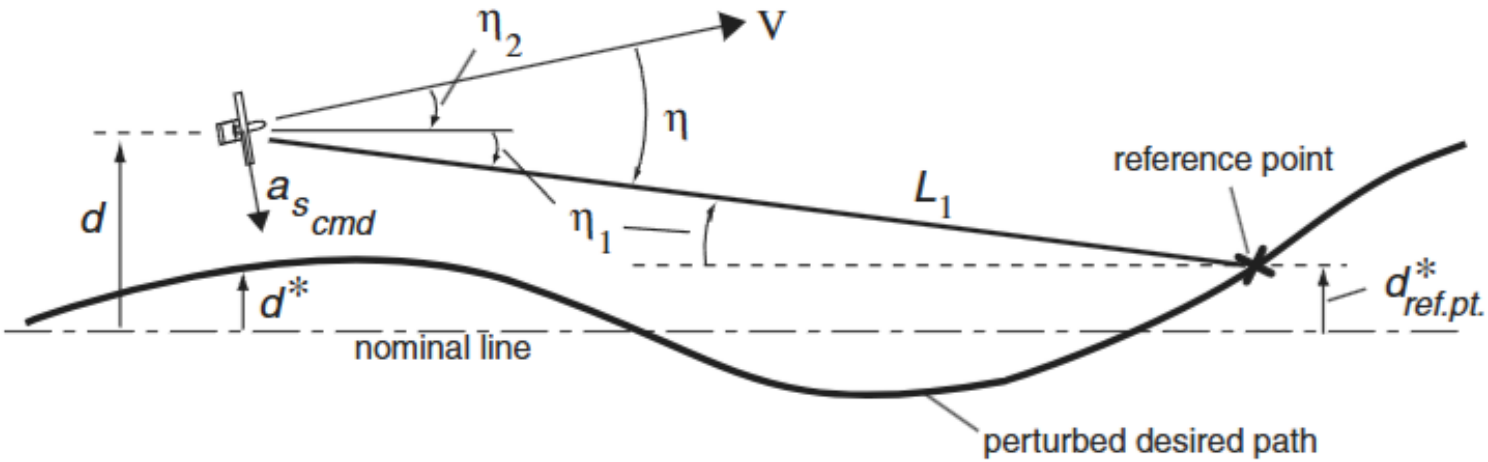

- From the guidance law: $a_{s_{cmd}} = 2\frac{V^2}{L_1}\sin\eta = 2\frac{V^2}{L_1}(\frac{d-d_{ref}}{L_1} + \frac{\dot{d}}{L_1})$. This resembles the form of a PD controller.
- So, $-\ddot{d} = 2\frac{V^2}{L_1}(\frac{d-d_{ref}}{L_1} + \frac{\dot{d}}{L_1})$

$$\boxed{\ddot{d} + 2\frac{V}{L_1}\dot{d} + 2\frac{V^2}{L_1^2}d = 2\frac{V^2}{L_1^2}d_{ref}} \quad (2)$$

Equations similar to a Spring Mass system with input d_{ref}

Linear Analysis

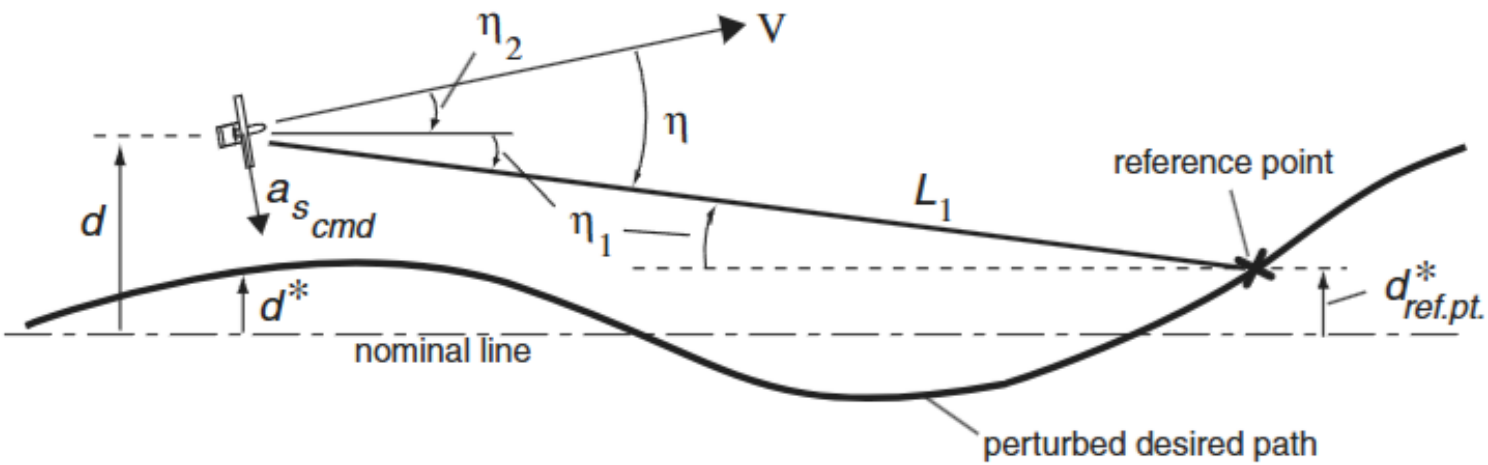

Taking the Laplace transform to find the transfer function of this system:

$$\frac{d(s)}{d^{\star}(s)} = \frac{\omega_n^2 e^{\tau s}}{s^2 + 2\zeta\omega_n s + \omega_n^2} \quad \text{where } \zeta = 0.707$$
$$\omega_n = \frac{\sqrt{2}V}{L_1} \text{ and } \frac{d_{ref}(s)}{d^{\star}(s)} = e^{\tau s} \text{ with } \tau \approx \frac{L_1}{V} \tag{3}$$

Linear Analysis

Testing this out for a sinusoidal input: $d^\star = A \sin \frac{2\pi x}{L_p}$. By varying L_p we can vary the frequency of the input.

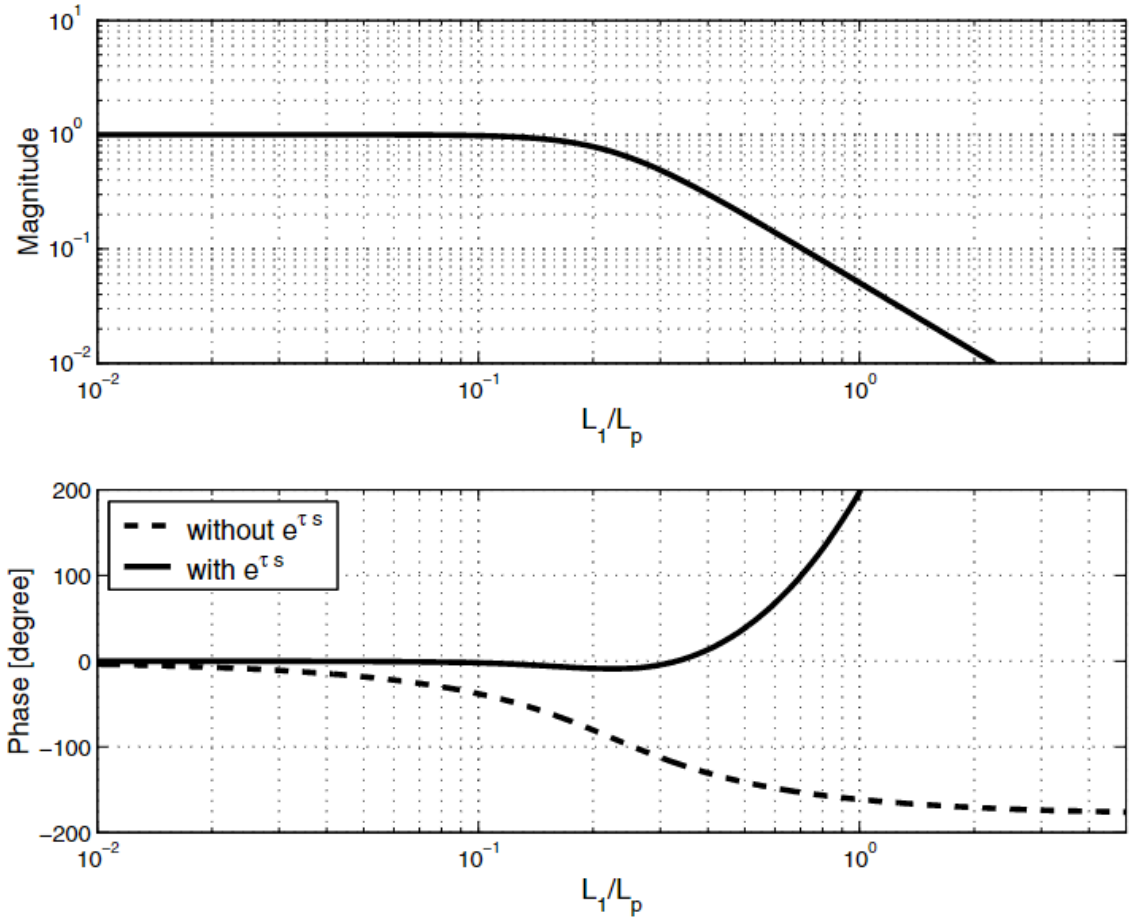

Figure 1: Bode Plots

Linear Analysis

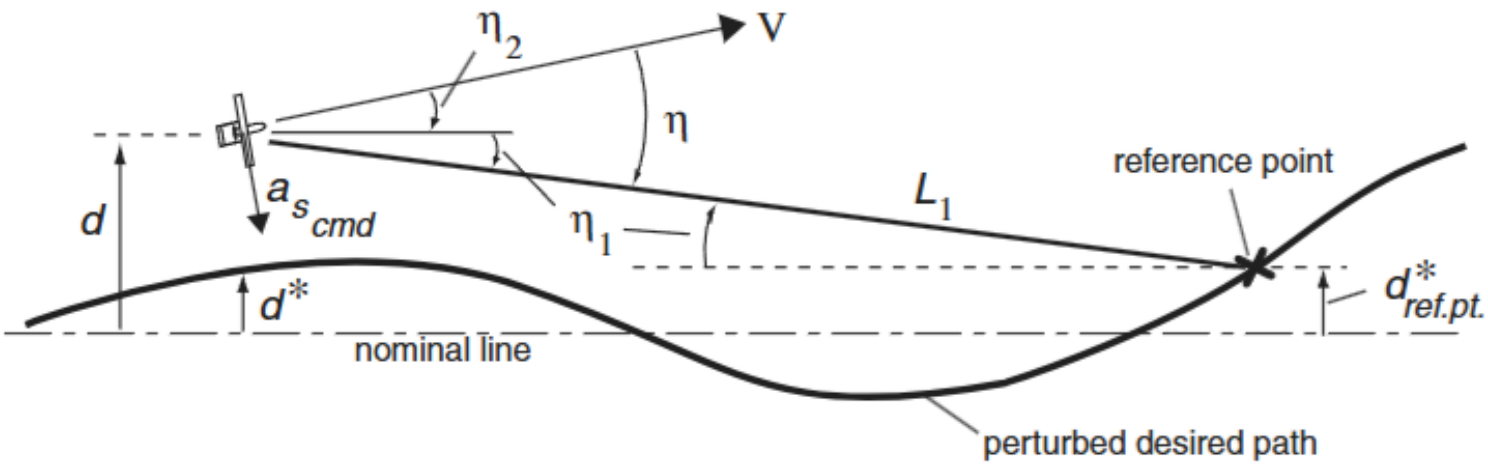

$$d^{\star} = A \sin \frac{2\pi x}{L_p}$$

This analysis indicates that if L_p is the wavelength of the highest frequency content in the desired path, then the look-ahead distance L_1 must be less than about $L_p/4.4$ if the vehicle is to follow the desired path accurately.

Simulation Results

Case 1: Circular path with wind disturbances.

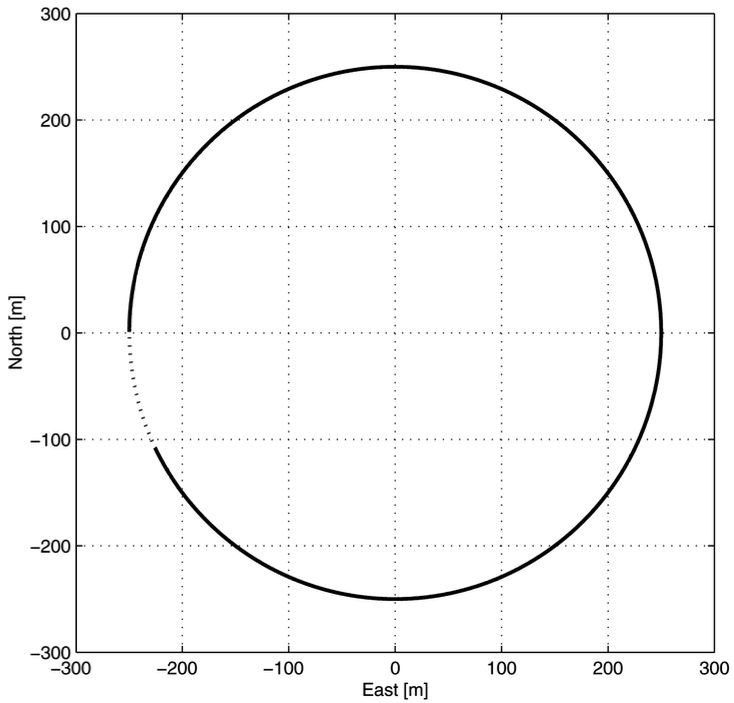

Figure 2: From the reference

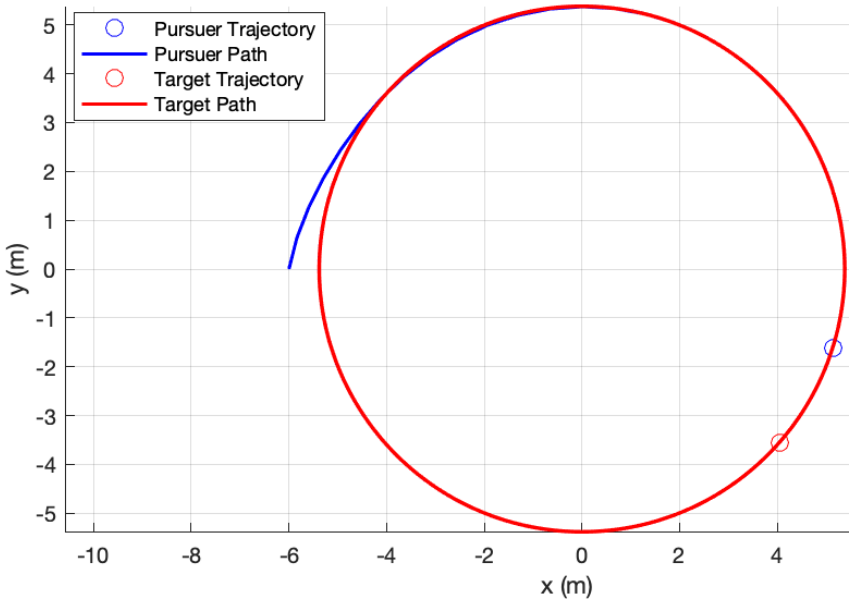

Figure 3: MATLAB Simulation

Simulation Results

Case 2: Linked circular path following.

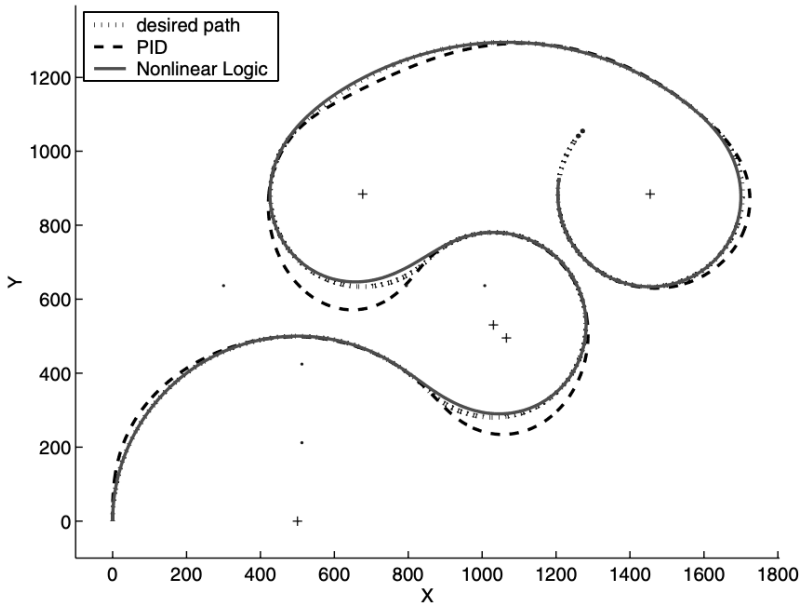

Figure 4: From the reference

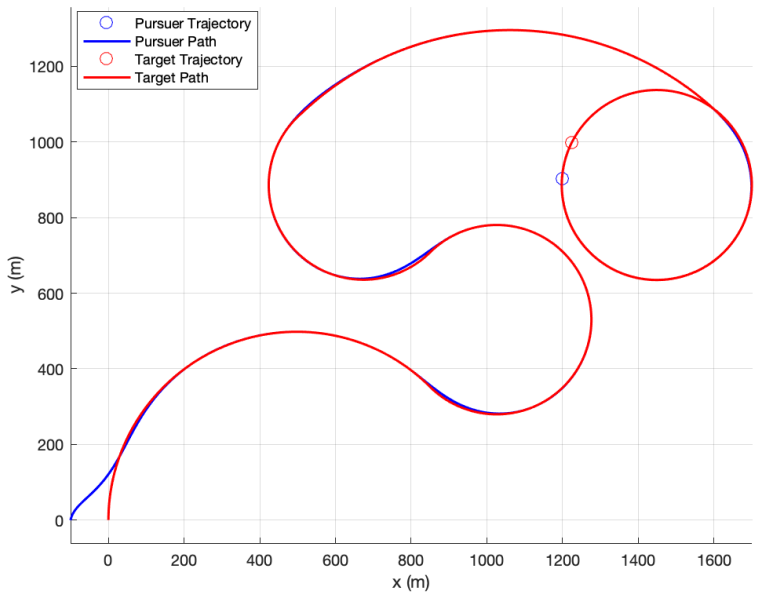

Figure 5: MATLAB Simulation

Simulation Results

Case 3: Trajectory generated using the 'randn' function.

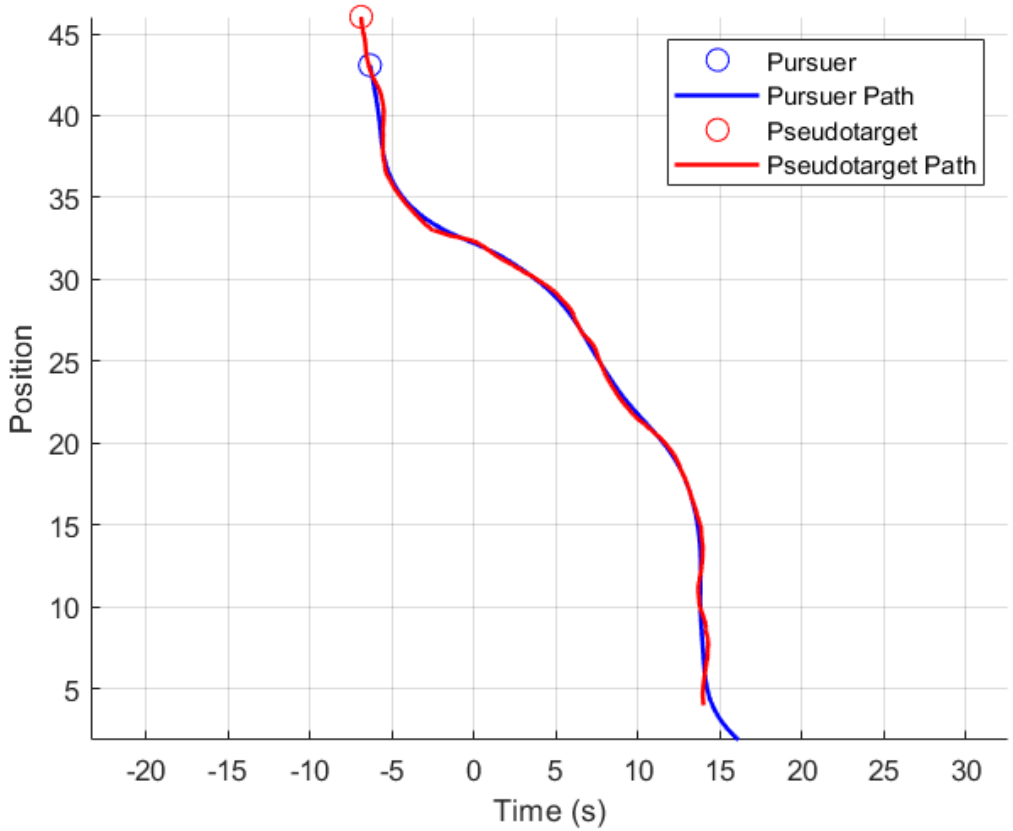

Figure 6: Tracking of a Randomly Generated Path

Stability Analysis

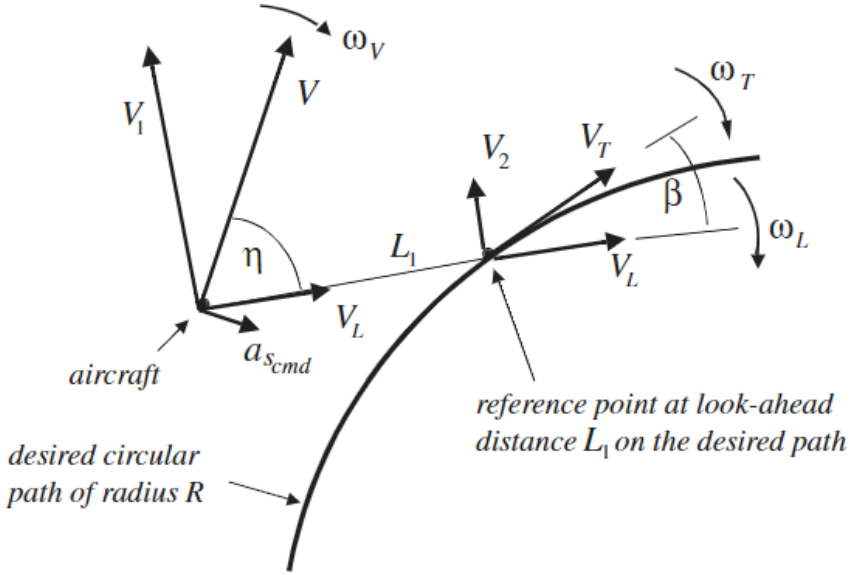

$$\dot{\eta} = \omega_L - \omega_V \ , \ \dot{\beta} = \omega_L - \omega_T$$

$$\omega_L = \frac{V_1 - V_2}{L_1} = \frac{V}{L_1}(\sin\eta - \cos\eta\tan\beta) \tag{4}$$

$$\omega_T = \frac{V_T}{R} = \frac{V\cos\eta}{R\cos\beta} \tag{5}$$

$$\omega_V = \frac{a_s}{V} = 2\frac{V}{L_1}\sin\eta \tag{6}$$

Stability Analysis

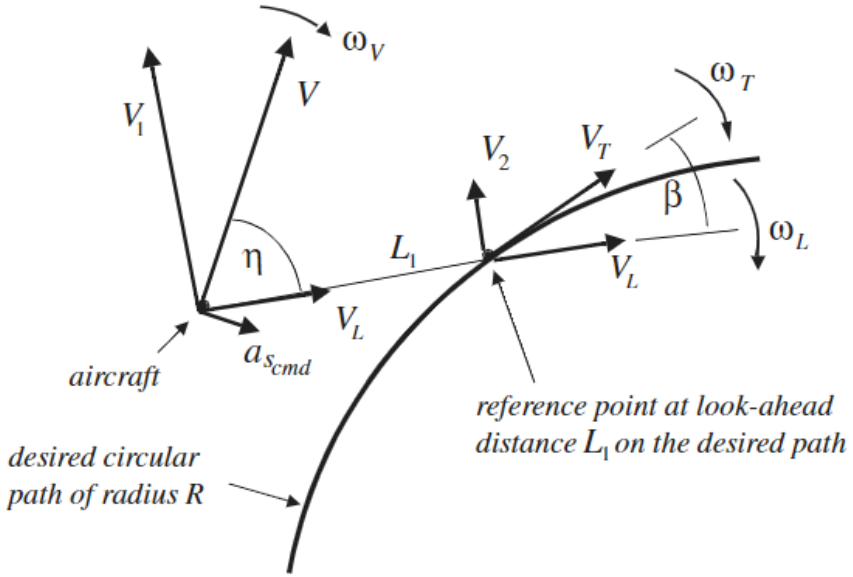

$$\dot{\eta} = -\frac{V}{L_1}(\sin\eta + \cos\eta\tan\beta) \tag{7}$$

$$\dot{\beta} = \frac{V}{L_1}(\sin\eta - \cos\eta\tan\beta) - \frac{V\cos\eta}{R\cos\beta} \tag{8}$$

Stability Analysis

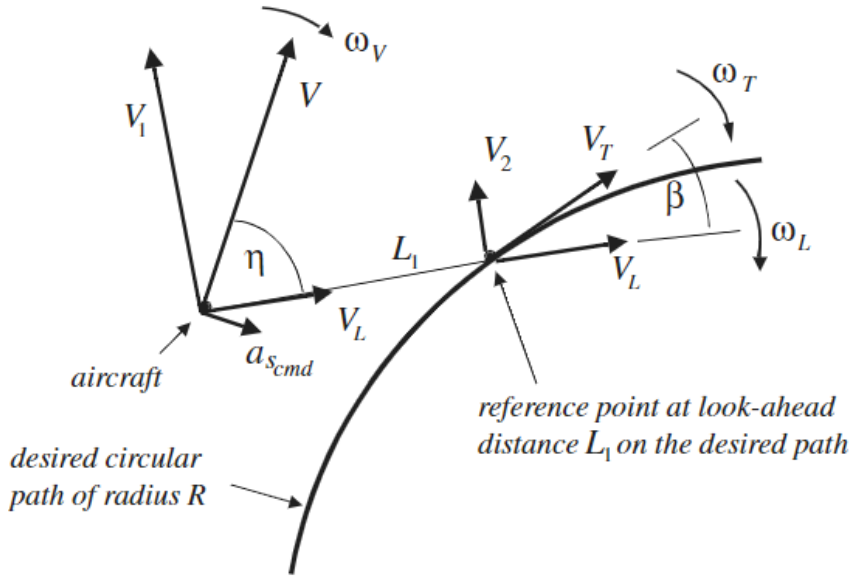

Equilibrium Points

$$\eta^\star = \sin^{-1}\left(\frac{L_1}{2R}\right) \tag{9}$$

$$\beta^\star = -\sin^{-1}\left(\frac{L_1}{2R}\right) \tag{10}$$

Stability Analysis

From the equation: $\dot{\eta} = -\frac{V}{L_1}(\sin\eta + \cos\eta \tan\beta)$ we can conclude the following:

- $\dot{\eta} > 0 \Leftrightarrow \eta < -\beta$
- $\dot{\eta} < 0 \Leftrightarrow \eta > -\beta$
- The curve that separates these 2 regions is given by $S_{\dot{\eta}} = \{\eta, \beta : \eta = -\beta\}$

Stability Analysis

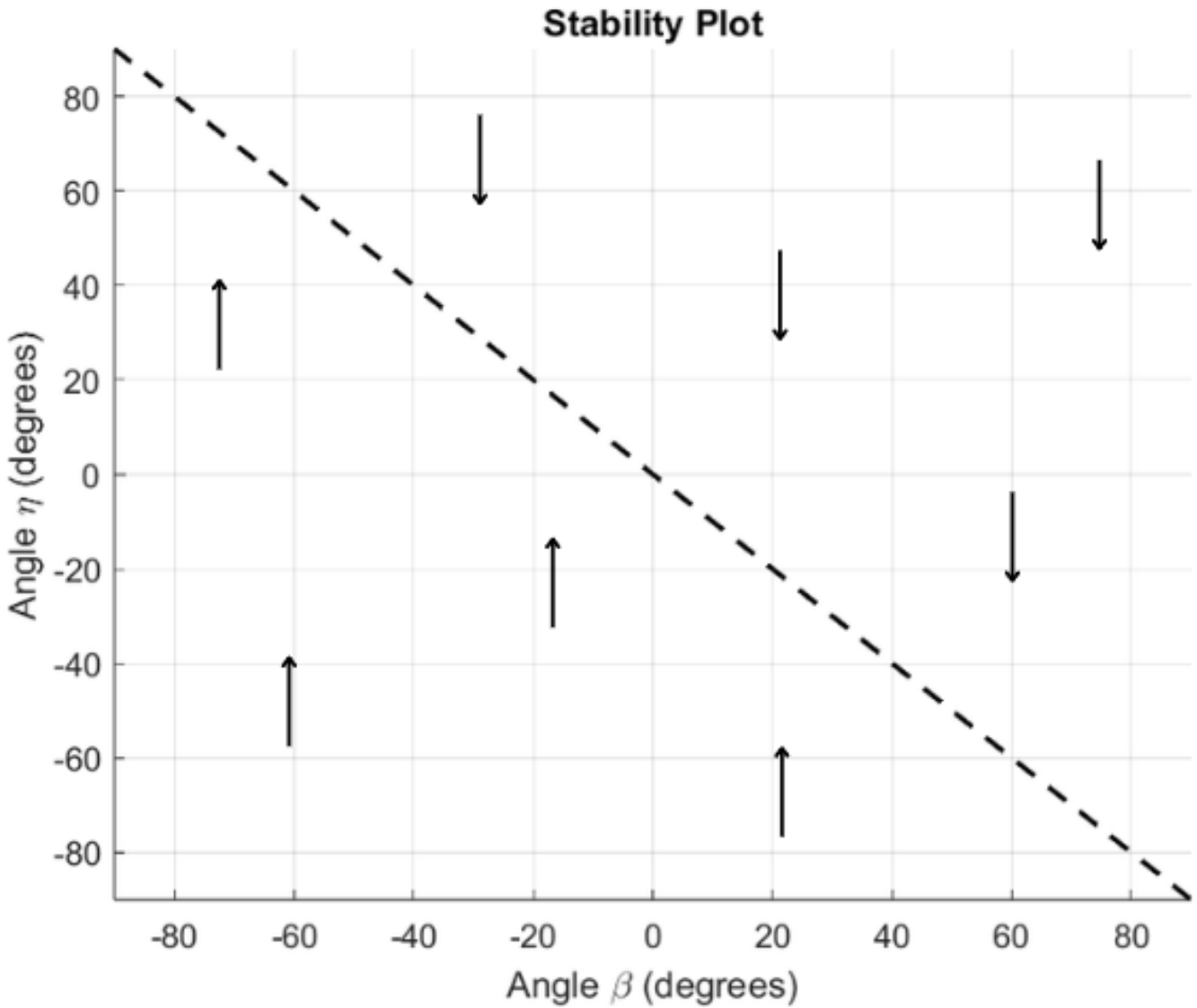

Figure 7: $\dot{\eta}$ trend across $S_{\dot{\eta}}$

Stability Analysis

From the equation: $\dot{\beta} = \frac{V}{L_1}(\sin\eta - \cos\eta\tan\beta) - \frac{V\cos\eta}{R\cos\beta}$ we can conclude the following:

- $\dot{\beta} > 0 \Leftrightarrow \beta < \eta - \sin^{-1}\left(\frac{L_1\cos\eta}{R}\right)$
- $\dot{\beta} < 0 \Leftrightarrow \beta > \eta - \sin^{-1}\left(\frac{L_1\cos\eta}{R}\right)$
- The curve that separates these 2 regions is given by $S_{\dot{\beta}} = \{\eta, \beta : \beta = \eta - \sin^{-1}\frac{L_1\cos\eta}{R}\}$

Similarly, we can define a separating region for $\dot{\eta} + \dot{\beta}$ as $S_{\dot{\eta}+\dot{\beta}} = \{\eta, \beta : \beta = \beta^{\star}\}$

Stability Analysis

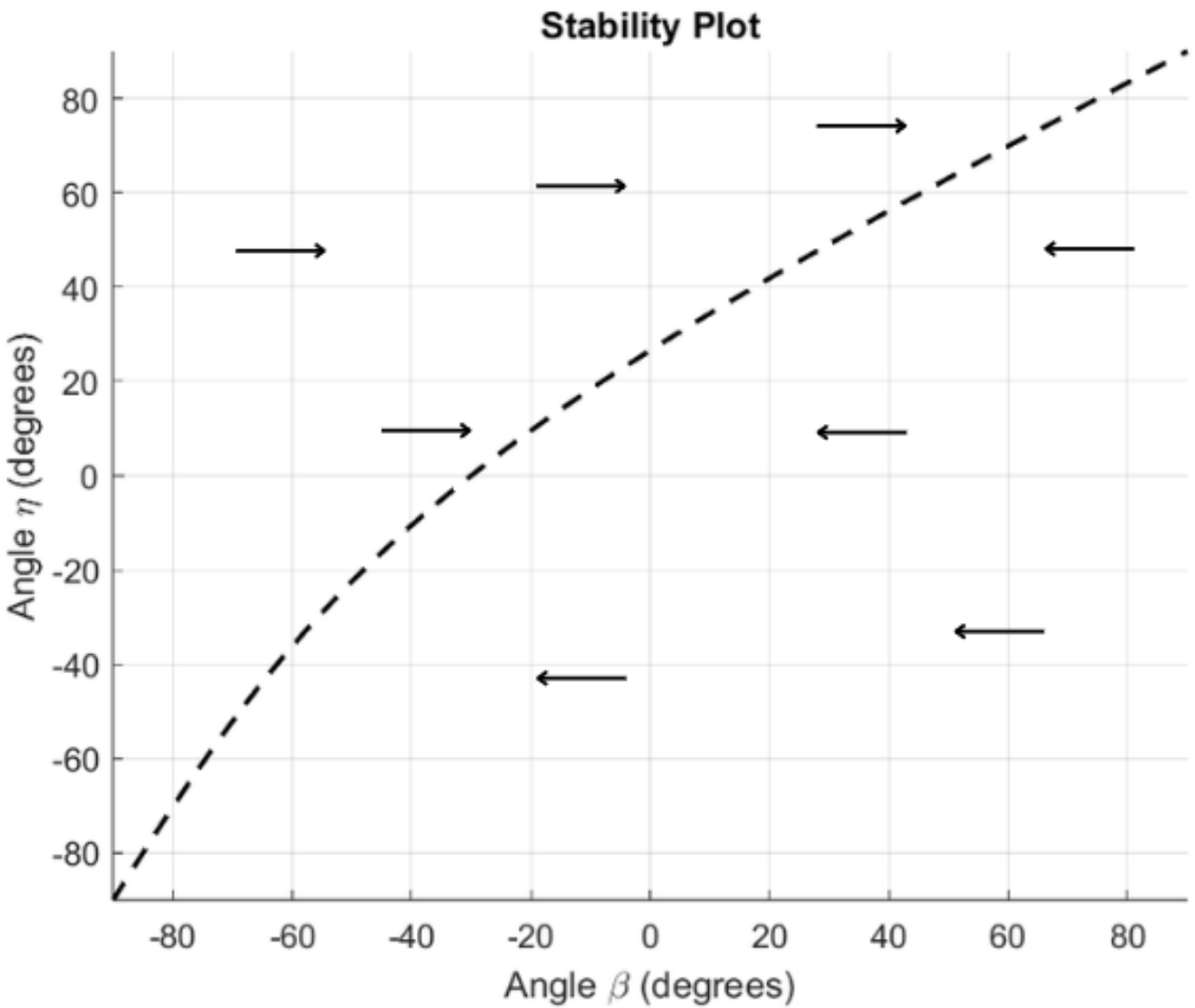

Figure 8: $\dot{\beta}$ trend across $S_{\dot{\beta}}$

Stability Analysis

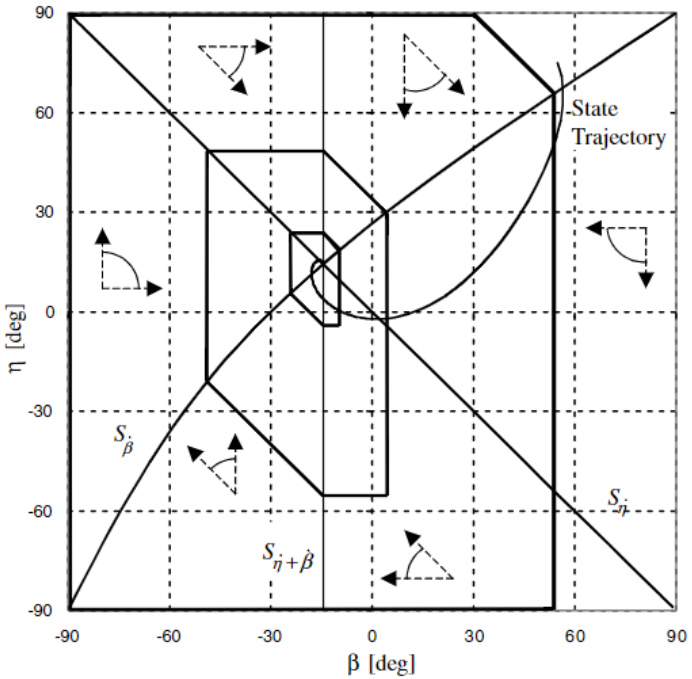

Figure 9: From the reference

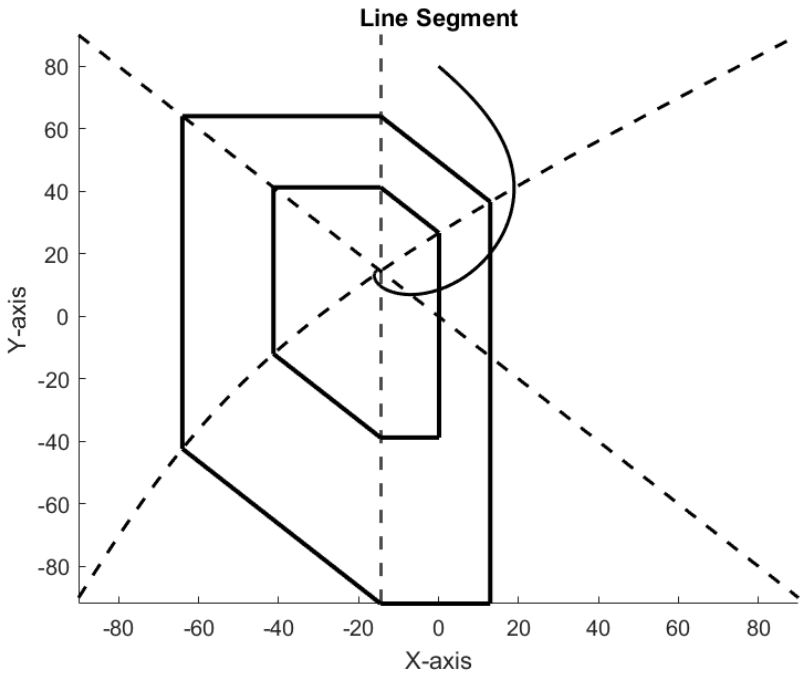

Figure 10: MATLAB Simulation

Stability Analysis

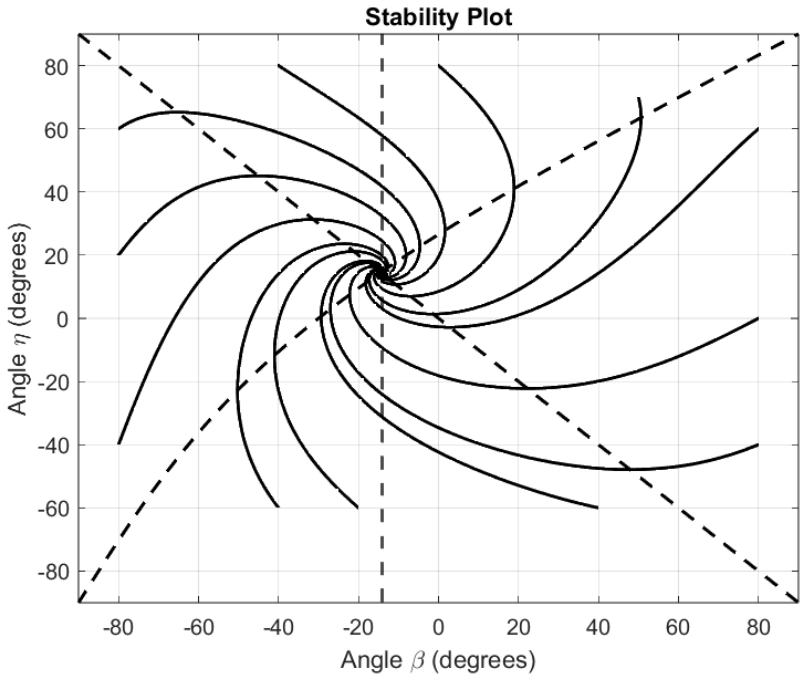

- We prove stability by proving that η and β tends towards the equilibrium values always.
- This, coupled with the fact that L_1 distance is constant, implies perfect tracking of trajectories.
- A similar stability analysis may be carried out in the presence of saturation effects.

Stability Analysis

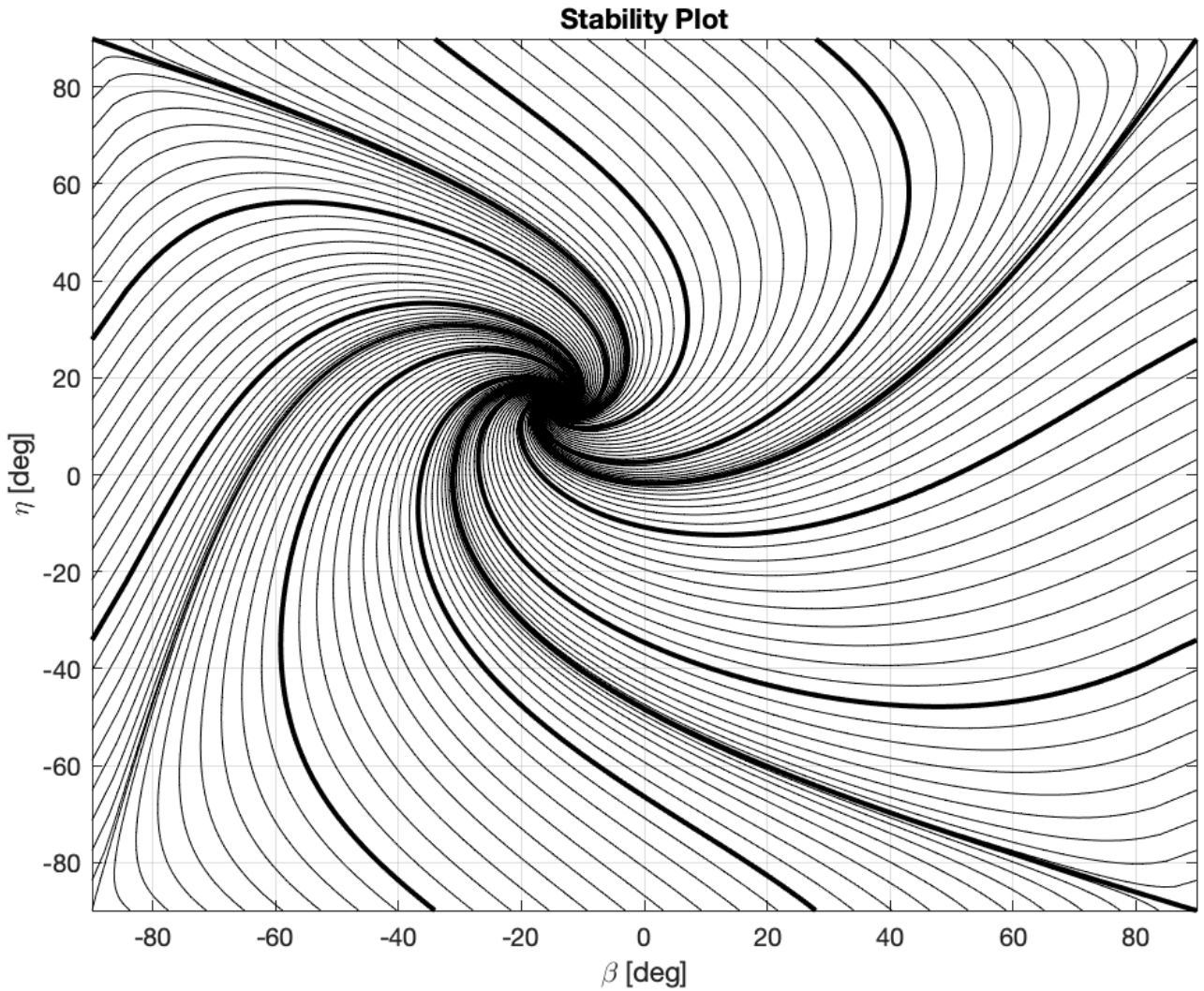

Flight Test Results

- The guidance algorithm was implemented and tested with the two UAVs constructed in the parent child unmanned air vehicle (PCUAV) project at MIT.
- Test parameters:
  - Nominal flight velocity $\simeq 25\ m/s$
  - $L_1 = 150\ m$
  - Average wind $= 5 \pm 1\ m/s$
- When the minivehicle flies along the circle the lateral displacement between the vehicle and the desired path remained within $\pm 2\ m$ for 75% of its flight time and within $\pm 3\ m$ for 96% of the flight time.
- Sensor errors in the onboard inertial system and wind variations are the most likely contributors to these remaining errors.

Flight Test Results

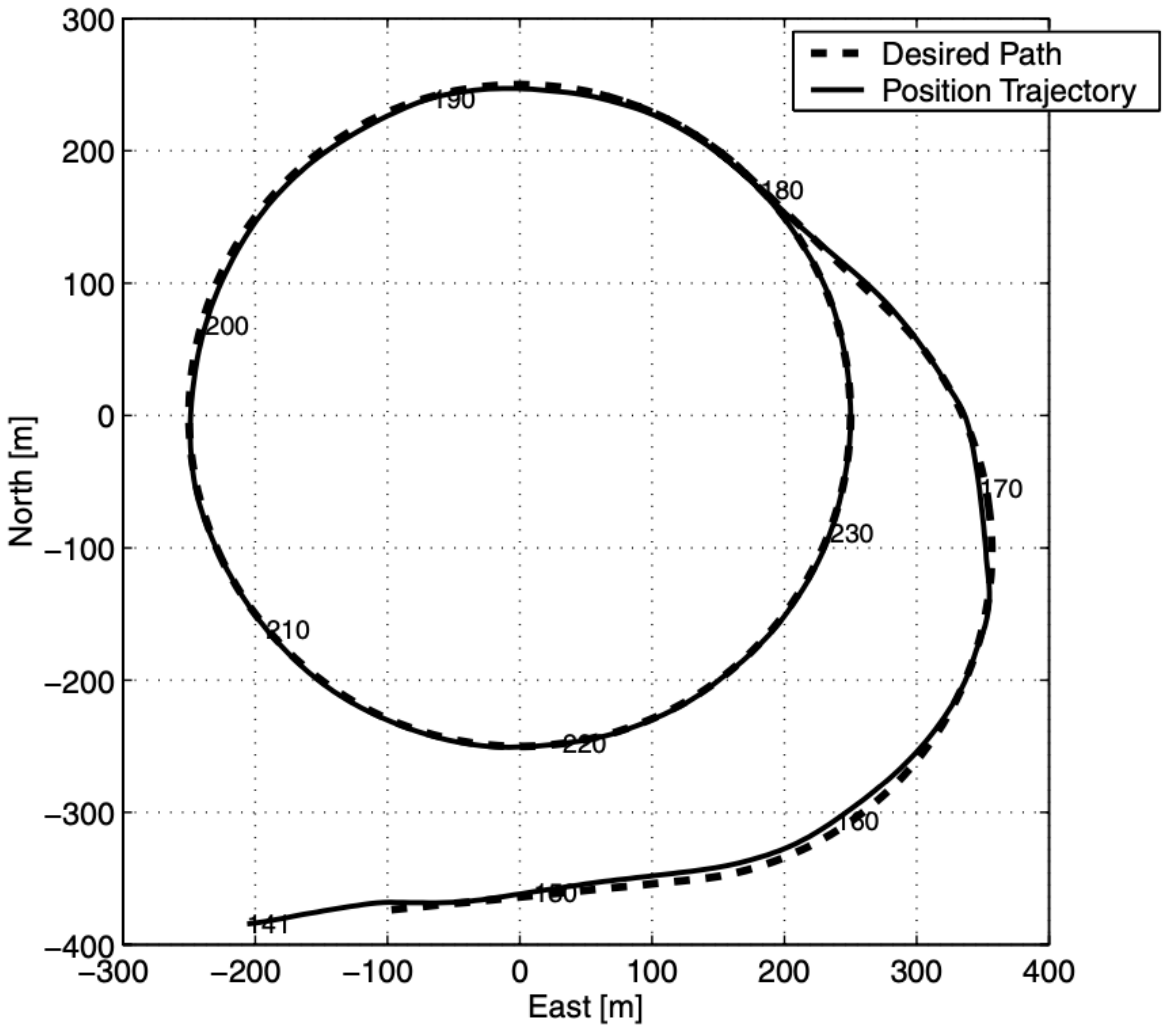

Figure 11: Flight Test Results

Improvement 1: Dynamic L_1

The shortcomings we observed in the paper are:

- No formal method is given to pick an appropriate L_1. Only have an upper bound of ($2 \times$ radius) has been given.
- A way to pick an L_1 when the pursuer is at a significant distance from the trajectory has also not been analyzed.
- While the paper analyzes the stability with reference to saturation effects, no study on the variation of a_P with time has been carried out.
- We aim to have a varying L_1 for the initial phase of flight such that the increase in the value of a_P is as smooth as possible.

Improvement 1: Dynamic L_1

To begin, we carry out the analysis on a circular reference trajectory.

- To avoid a sudden jump in a_P, we want a_P to start from its minimum possible value while employing the guidance law.
- We start by checking every point on the trajectory and find the point at which minimum acceleration is achieved. This gives the initial pseudotarget.
- Using this minimum acceleration we step forward in time and similarly pick the minumum acceleration for the next point.
- We find that the acceleration gradually increases and L_1 decreases.
- The process may be stopped when the desired L_1 is achieved and the guidance law with constant L_1 can be applied hereafter.

Improvement 1: Dynamic L_1

Simulation parameters and results:

- $x_{P_0} = -10\ m$, $y_{P_0} = 1\ m$
- $\alpha_{P_0} = 60°$, $V = 10\ m/s$
- $R = 3\ m$, centre at origin.
- To achieve $L_1 = 7.1\ m$ starting from the intial point, an acceleration of over 26 m/s^2 is needed. However, using the dynamic L_1, $L_1 = 6\ m$ can be achieved with a maximum a_P of under 13.44 m/s^2.

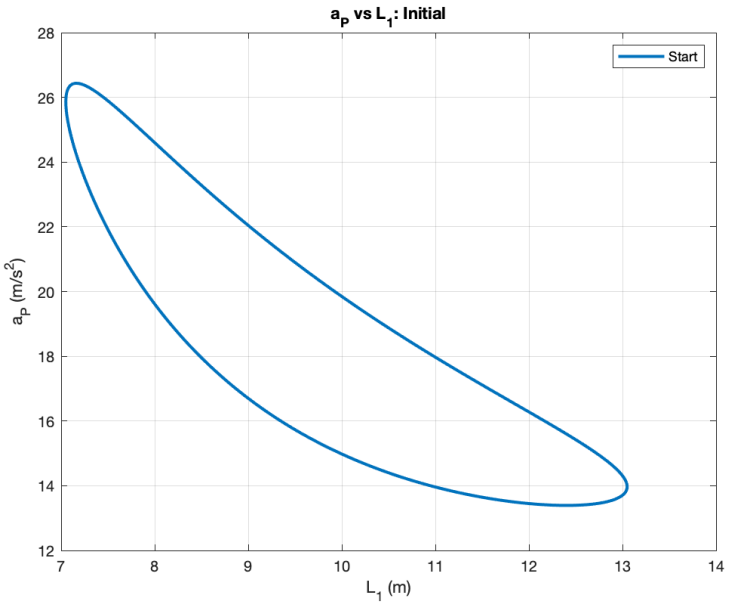

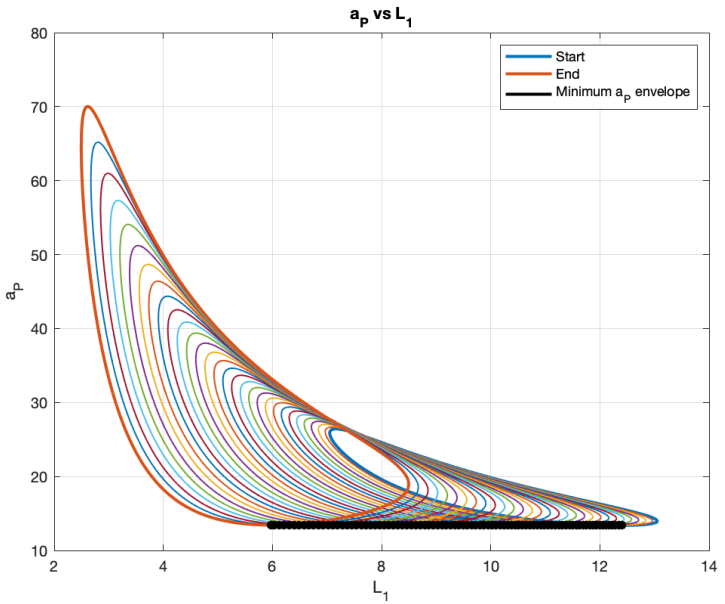

Improvement 1: Dynamic L_1

The following plots are for the variation of a_P and L_1 with time.

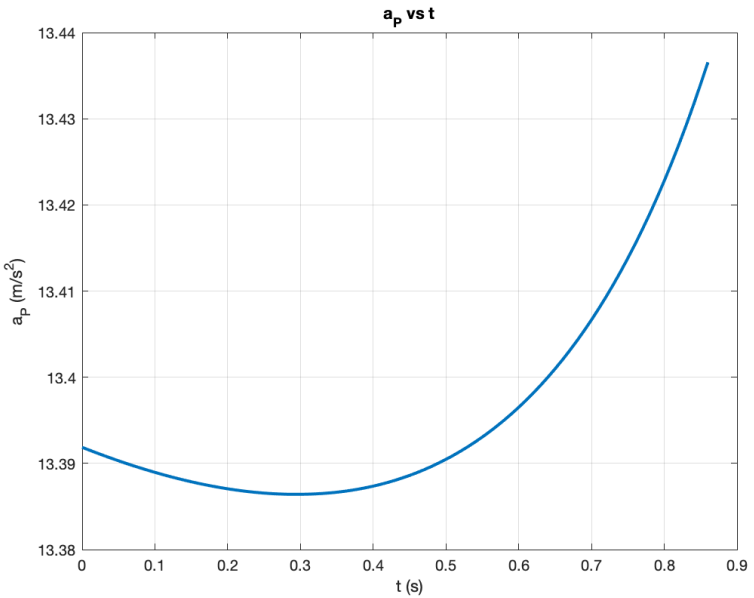

Figure 12: a_P vs. time

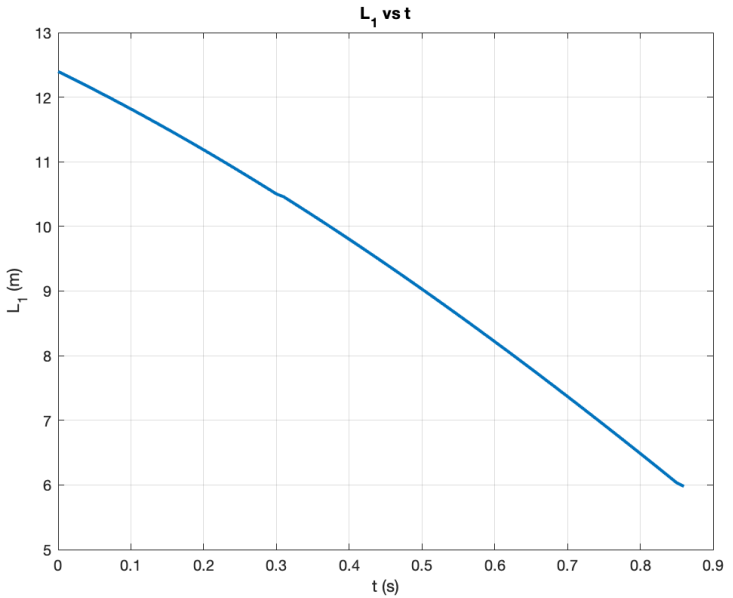

Figure 13: L_1 vs. time

Improvement 2: Multiple Look Ahead Points

Motivation: Whenever the desired path involves $\ddot{\alpha}_t$, while the pursuer tries to maintain the constant L_1 distance, it does not strictly follow the desired path.

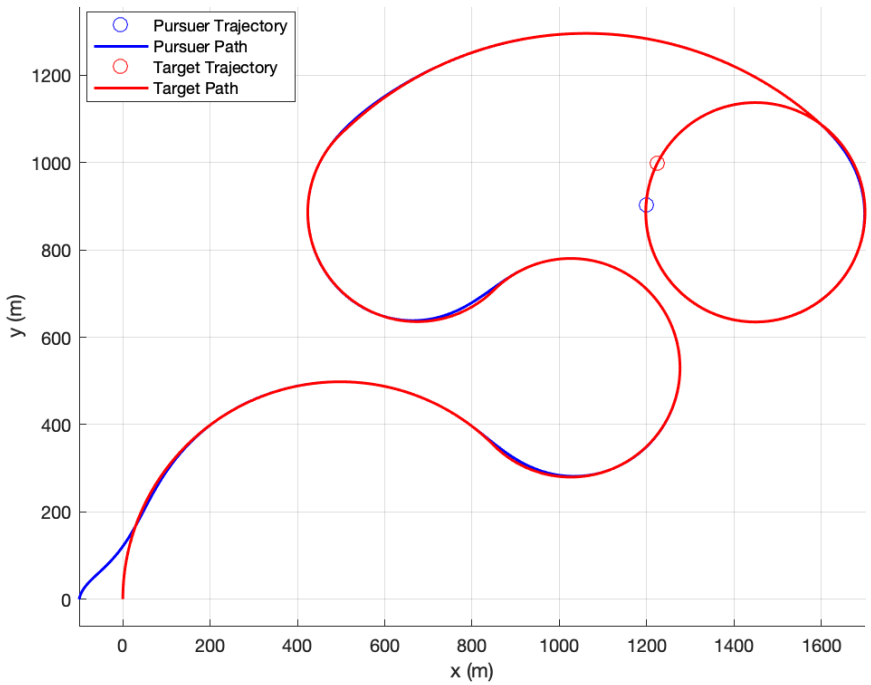

Figure 14: Inexact Path Following

Improvement 2: Multiple Look Ahead Points

To solve this issue, a formulation involving multiple look ahead points is considered.

- The resultant lateral acceleration of the pursuer is taken as a weighted mean of the acceleration stemming from each look-ahead point.

$$a_{s_{cmd}} = \frac{\sum_{i=1}^{n} 2 w_i \frac{V^2}{L_i} \sin \eta_i}{\sum_{i=1}^{n} w_i} \tag{11}$$

- Intuition behind this formulation is the desire to capture more information about the path followed by the pseudo-target.
- By weighing the nearer points more, one can track the desired path more tightly.
- An interesting avenue to explore could be formulating a dynamic weight change that optimizes a particular cost function (e.g. Control Effort, Tracking Inaccuracy)

Improvement 2: Multiple Look Ahead Points

Improved Tracking

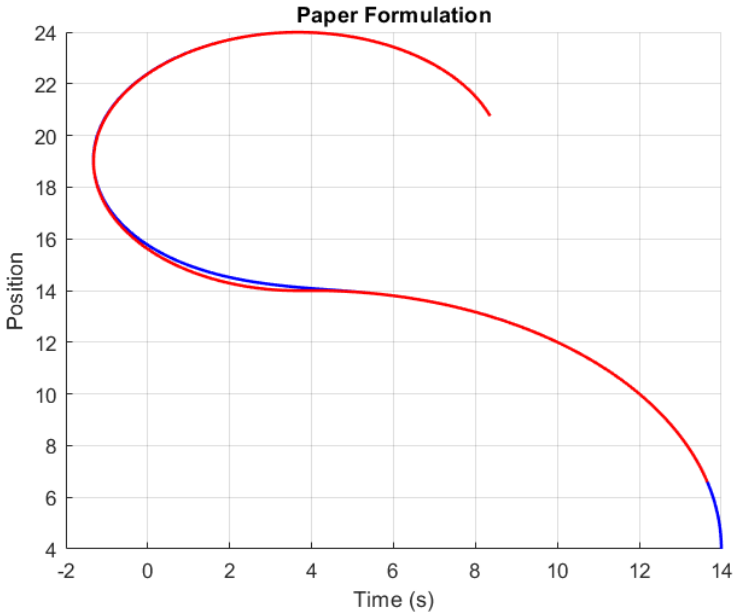

Figure 15: 1 Look Ahead Point

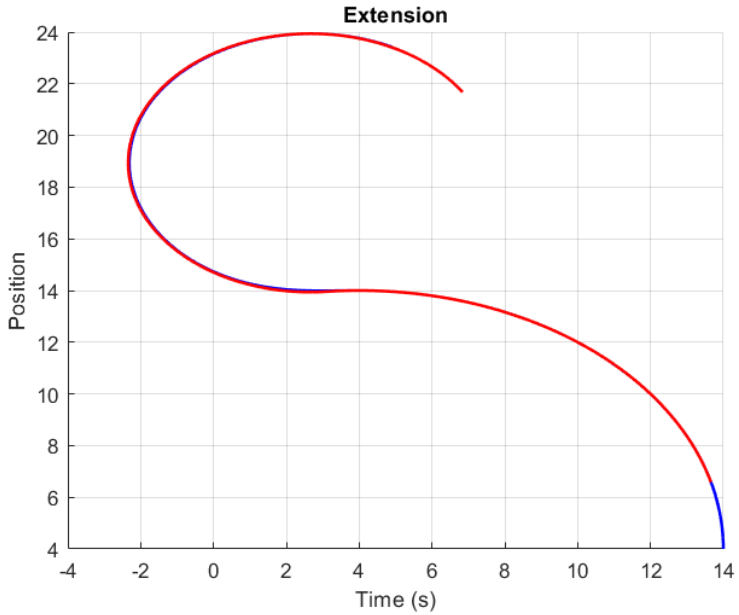

Figure 16: 2 Look Ahead Points

Conclusion

We find that the nonlinear guidance method formulated in this paper offers significant advantages over the traditional linear technique in the presence of wind disturbances and in terms of stability.

Reference: Park, Sanghyuk et al. "Performance and Lyapunov Stability of a Nonlinear Path Following Guidance Method." Journal of Guidance Control and Dynamics 30 (2007): 1718-1728.